

# 1 Microbiotyping the sinonasal microbiome

2 Ahmed Bassiouni<sup>1</sup>, Sathish Paramasivan<sup>1</sup>, Arron Shiffer<sup>2</sup>, Matthew R Dillon<sup>2</sup>, Emily K Cope<sup>2</sup>,  
3 Clare Cooksley<sup>1</sup>, Mahnaz Ramezanpour<sup>1</sup>, Sophia Moraitis<sup>1</sup>, Mohammad Javed Ali<sup>3</sup>, Benjamin  
4 Bleier<sup>4</sup>, Claudio Callejas<sup>5</sup>, Marjolein E Cornet<sup>6</sup>, Richard G Douglas<sup>7</sup>, Daniel Dutra<sup>8</sup>, Christos  
5 Georgalas<sup>6</sup>, Richard J Harvey<sup>9,10</sup>, Peter H Hwang<sup>11</sup>, Amber U Luong<sup>12</sup>, Rodney J Schlosser<sup>13</sup>,  
6 Pongsakorn Tantilipikorn<sup>14</sup>, Marc A Tewfik<sup>15</sup>, Sarah Vreugde<sup>1</sup>, Peter-John Wormald<sup>1</sup>, J Gregory  
7 Caporaso<sup>2</sup>, and Alkis J Psaltis<sup>1</sup>

8 <sup>1</sup> Department of Otolaryngology, Head and Neck Surgery, University of Adelaide, Adelaide, Australia

9 <sup>2</sup> Pathogen and Microbiome Institute, Northern Arizona University, Arizona, USA

10 <sup>3</sup> Dacryology Service, LV Prasad Institute, Hyderabad, India

11 <sup>4</sup> Department of Otolaryngology, Massachusetts Eye and Ear Infirmary, Harvard Medical School, Boston, USA

12 <sup>5</sup> Department of Otolaryngology, Pontificia Universidad Catolica de Chile, Santiago, Chile

13 <sup>6</sup> Department of Otorhinolaryngology, Amsterdam UMC, Amsterdam, The Netherlands

14 <sup>7</sup> Department of Surgery, University of Auckland, Auckland, New Zealand

15 <sup>8</sup> Department of Otorhinolaryngology, University of Sao Paulo, Sao Paulo, Brazil

16 <sup>9</sup> Department of Otolaryngology, Rhinology and Skull base, University of New South Wales, Sydney, Australia

17 <sup>10</sup> Faculty of Medicine and Health sciences, Macquarie University, Sydney, Australia

18 <sup>11</sup> Department of Otolaryngology -Head and Neck Surgery, Stanford University, Stanford, California, USA

19 <sup>12</sup> Department of Otolaryngology -Head and Neck Surgery, University of Texas, Texas, USA

20 <sup>13</sup> Department of Otolaryngology, Medical University of South Carolina, Charleston, South Carolina, USA

21 <sup>14</sup> Department of Otorhinolaryngology, Faculty of Medicine, Siriraj Hospital, Mahidol University, Bangkok, Thailand

22 <sup>15</sup> Department of Otolaryngology - Head and Neck Surgery, McGill University, Montreal, Canada

## 23 Corresponding author:

24 Associate Professor Alkis J Psaltis

25 3C (Department of Otolaryngology, Head and Neck Surgery)

26 The Queen Elizabeth Hospital

27 28 Woodville Rd  
28 Woodville South, SA 5011  
29 Australia  
30 Email: alkis.psaltis@adelaide.edu.au  
31 Phone: +61 08 8222 7158  
32 Fax: +61 08 8222 7419

33 **Funding information, Disclosures and Conflicts of Interest (COI):**

34 Mohammad Javed Ali:  
35 Receives royalties from Springer for his treatise “Principles and Practice of Lacrimal Surgery” and “Atlas  
36 of Lacrimal Drainage Disorders”.  
37 No conflict of interest relevant to this study.

38 Ahmed Bassiouni, Clare Cooksley, Mahnaz Ramezanpour, Sophia Moraitis:  
39 No conflict of interest to declare.

40 Benjamin Bleier:  
41 Grant Funding: R01 NS108968-01 NIH/NINDS (Bleier PI) – This isn’t relevant to this study.  
42 Consultant for: Gyrus ACMI Olympus, Canon, Karl Storz, Medtronic, and Sinopsys.  
43 Equity: Cerebent, Inc, Arrinex.  
44 COI: None relevant to this study.

45 Claudio Callejas:  
46 No conflict of interest to declare.

47 J Gregory Caporaso, Matthew R Dillon, Arron Shiffer:  
48 No conflicts of interest to declare. This work was funded in part by National Science Foundation Award  
49 1565100 to JGC.

50    Emily K Cope:

51    Financial information: This work was partially funded under the State of Arizona Technology and

52    Research Initiative Fund (TRIF), administered by the Arizona Board of Regents, through Northern

53    Arizona University.

54    No relevant disclosures or COI.

55    Marjolein E Cornet:

56    No financial relationships or sponsors. No conflicts of interests.

57    Richard G Douglas:

58    Received consultancy fees from Lyra Therapeutics and is a consultant for Medtronic. These are not

59    relevant to this study.

60    Daniel Dutra:

61    No conflict of interest to declare.

62    Richard J Harvey:

63    Consultant with Medtronic, Olympus and NeilMed pharmaceuticals. He has also been on the speakers'

64    bureau for Glaxo-Smith-Kline, Seqiris and Astra-Zeneca.

65    No direct conflict of interest to declare.

66    Christos Georganas:

67    No conflicts of interest to declare.

68    Peter H Hwang:

69    Financial Relationships: Consultancies with Arrinex, Bioinspire, Canon, Lyra Therapeutics, Medtronic,

70    Tivic.

71    Conflicts of Interest: None.

72    Amber U Luong:  
73    Serves as a consultant for Aerin Medical (Sunnyvale, CA), Arrinex (Redwood City, CA), Lyra  
74    Therapeutics (Watertown, MA), and Stryker (Kalamazoo, MI) and is on the advisory board for  
75    ENTvantage (Austin, TX).  
76    Her department receives funding from Genetech/Roche (San Francisco, CA) and AstraZeneca  
77    (Cambridge, England).  
78    No COI to declare related to this study.

79    Sathish Paramasivan:  
80    Supported by a Garnett Passe and Rodney Williams Memorial Foundation Academic Surgeon Scientist  
81    Research Scholarship.  
82    No conflicts of interest to declare.

83    Alkis J Psaltis:  
84    Consultant for Aerin Devices and ENT technologies and is on the speakers' bureau for Smith and  
85    Nephew. Received consultancy fees from Lyra Therapeutics. These are not relevant to this study.

86    Rodney J Schlosser:  
87    Grant support from OptiNose, Entellus, and IntersectENT (not relevant to this study). Consultant for  
88    Olympus, Meda, and Arrinex (not relevant to this study).

89    Pongsakorn Tantilipikorn:  
90    No financial disclosures or conflict of interest.

91    Marc A Tewfik:  
92    Principal Investigator: Sanofi, Roche/Genentech, AstraZeneca.  
93    Speaker/Consultant: Stryker, Ondine Biomedical, Novartis, MEDA, Mylan.  
94    Royalties for book sales: Thieme.

95 Sarah Vreugde:

96 No conflicts of interest relevant to this study.

97 Peter-John Wormald:

98 Receives royalties from Medtronic, Integra, and Scopis, and is a consultant for NeilMed. These are not  
99 relevant to this study.

100

101 **Abstract**

102 This study offers a novel description of the sinonasal microbiome, through an unsupervised machine  
103 learning approach combining dimensionality reduction and clustering. We apply our method to the  
104 International Sinonasal Microbiome Study (ISMS) dataset of 410 sinus swab samples. We propose three  
105 main sinonasal ‘microbiotypes’ or ‘states’: the first is *Corynebacterium*-dominated, the second is  
106 *Staphylococcus*-dominated, and the third dominated by the other core genera of the sinonasal microbiome  
107 (*Streptococcus*, *Haemophilus*, *Moraxella*, and *Pseudomonas*). The prevalence of the three microbiotypes  
108 studied did not differ between healthy and diseased sinuses, but differences in their distribution were  
109 evident based on geography. We also describe a potential reciprocal relationship between  
110 *Corynebacterium* species and *Staphylococcus aureus*, suggesting that a certain microbial equilibrium  
111 between various players is reached in the sinuses. We validate our approach by applying it to a separate  
112 16S rRNA gene sequence dataset of 97 sinus swabs from a different patient cohort. Sinonasal  
113 microbiotyping may prove useful in reducing the complexity of describing sinonasal microbiota. It may  
114 drive future studies aimed at modeling microbial interactions in the sinuses and in doing so may facilitate  
115 the development of a tailored patient-specific approach to the treatment of sinus disease in the future.

116 **Keywords**

117 microbiome, sinus, next-generation sequencing, 16S rRNA gene, chronic rhinosinusitis, microbiotype

118

119 **MAIN TEXT**

120 Chronic rhinosinusitis (CRS) is a heterogenous, multi-factorial inflammatory disorder with a complex and  
121 incompletely understood aetiopathogenesis.<sup>1</sup> A potential role of the sinonasal microbiome and its  
122 “dysbiosis” in CRS pathophysiology has recently gained increased interest. The nature of the microbial  
123 dysbiosis and its role in disease causation and progression however remains unclear, with conflicting  
124 findings from the small sinonasal microbiome studies published thus far.

125 We recently reported the findings of our multi-national, multicenter “International Sinonasal Microbiome  
126 Study” or ISMS.<sup>2</sup> This study, the largest and most diverse of its kind to date, attempted to address many  
127 of the limitations of the smaller previous studies, by standardizing collection, processing and analysis of  
128 the samples. Furthermore, its large sample size and multinational recruitment, meant that it was more  
129 likely to capture geographical and centre-based differences if present. A recent meta-analysis of published  
130 sinonasal 16S rRNA sequences revealed that the largest proportion of variance was attributed to  
131 differences between studies,<sup>3</sup> highlighting a role for performing a large multi-centre study that employed  
132 a unified methodology.

133 Contrary to the findings of previous studies, our international cohort showed no significant differences in  
134 alpha or beta diversity between the three groups of patients analyzed: healthy control patients without  
135 CRS and the two phenotypes of CRS patients, those with polyps (CRSwNP) and those without  
136 (CRSsNP). The study however revealed a potential grouping of samples as demonstrated on beta diversity  
137 exploratory analysis.<sup>2</sup> Accordingly, we hypothesized that the bacteriology of the sinuses could be  
138 categorized into various clusters of similar compositions. We inquired whether these potential groups  
139 would aid in describing the sinonasal microbial composition of patients or associate with clinical features.  
140 Similar attempts performed on gut microbiota in healthy individuals were termed *enterotyping*.<sup>4</sup> The  
141 clinical relevance of gut enterotypes remain the topic of research, and sometimes controversy. A previous  
142 exploration of clusters of sinus microbiota in patients was performed by Cope et al.<sup>5</sup> in which the authors

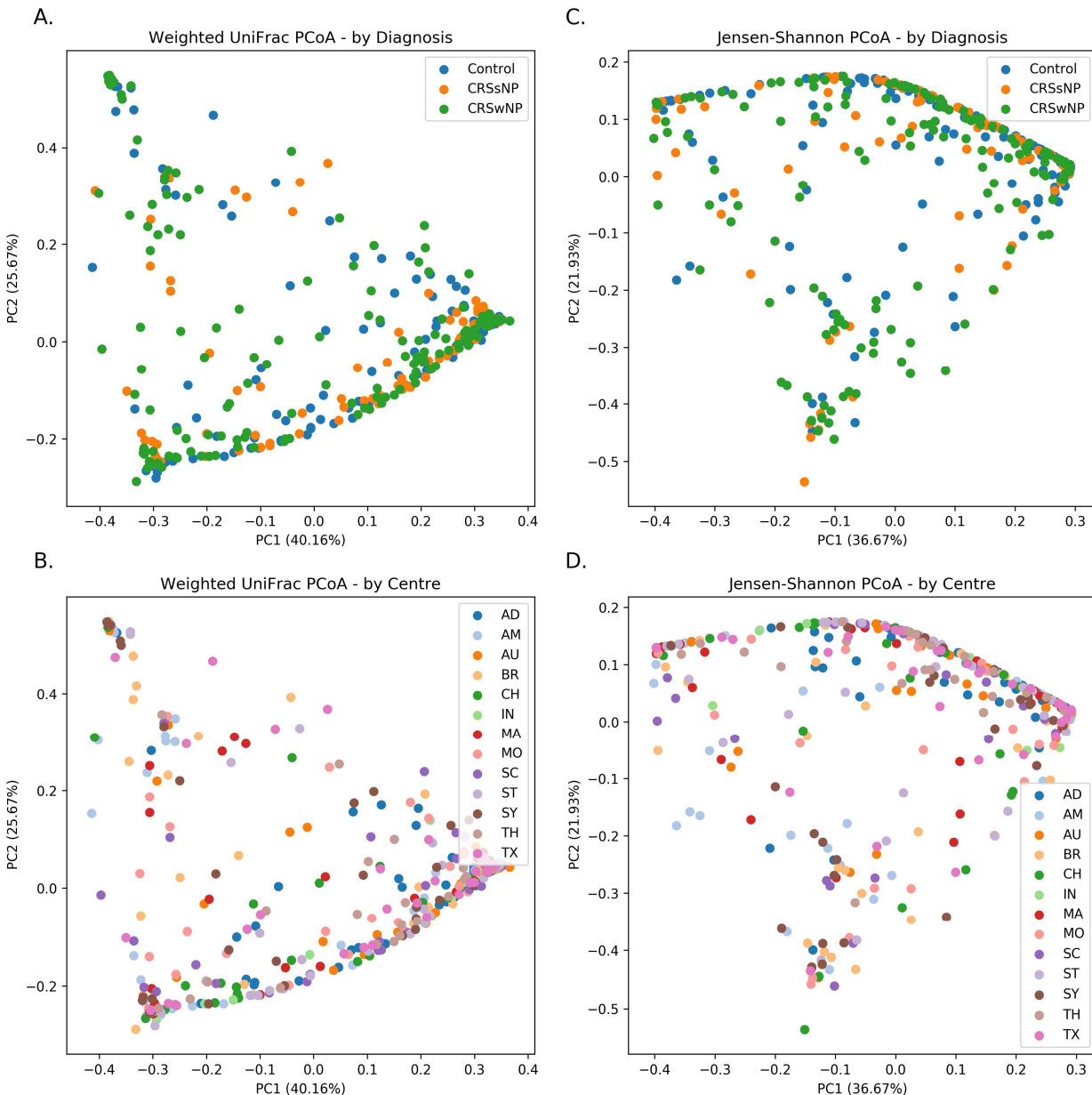
143 reported four compositionally distinct sinonasal microbial community states; the largest group of patients  
144 were dominated by a continuum of Staphylococcaceae and Corynebacteriaceae demonstrating a  
145 reciprocal relationship.<sup>5</sup>

146 In this manuscript, we attempt “microbiotyping” to explain interpatient heterogeneity of the bacterial  
147 communities in the paranasal sinuses, and are the first to describe “sinonasal microbiotypes” across the  
148 first large, multi-centre cohort of individuals with and without CRS. We model our analysis on previous  
149 attempts of enterotyping the gut microbiome. We then describe the composition of these microbiotypes,  
150 explore potential clinical associations and validate microbiotyping on a separate sinus microbiome  
151 dataset.

152

## 153 RESULTS

### 154 Basic characteristics of the study cohort and beta diversity plots



155

156 **Figure 1: Beta diversity ordination plots.**

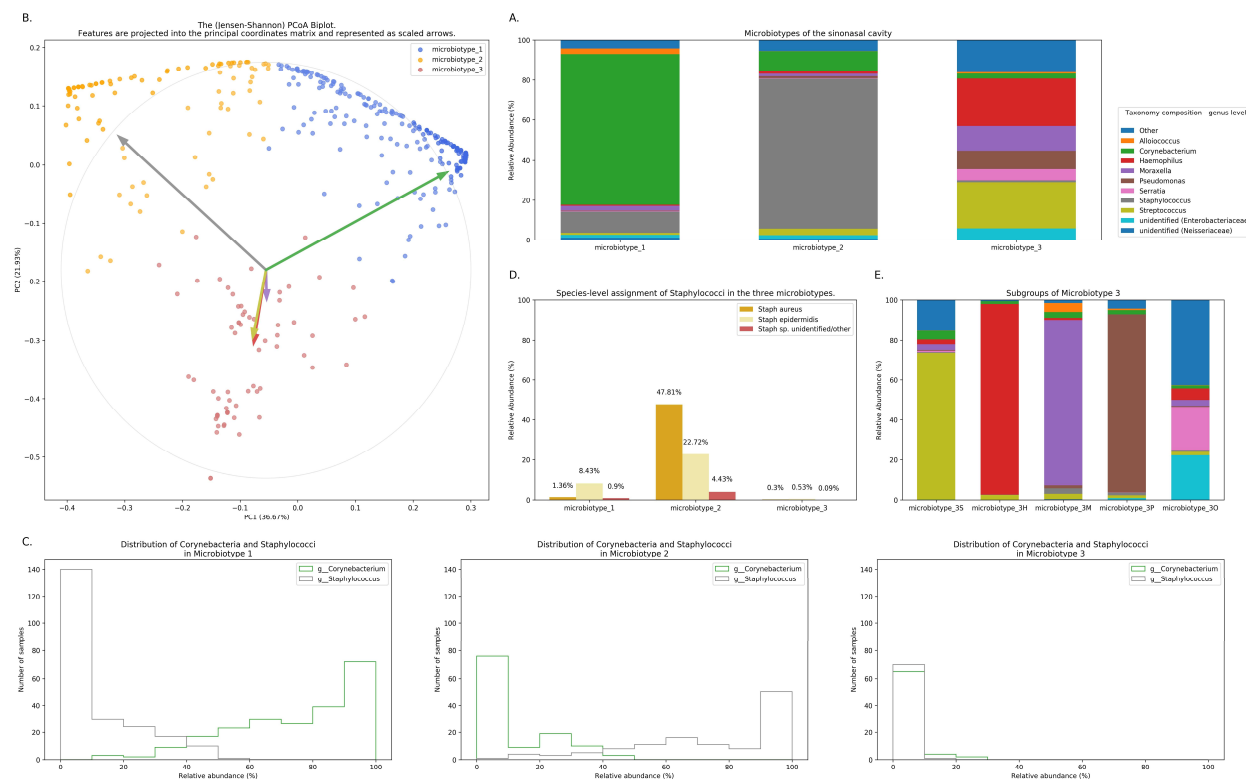
157 The main ISMS study cohort was described in our previous publication.<sup>2</sup> In brief, 410 samples were

158 included in the analysis collected from 13 centres representing 5 continents. These samples are distributed

159 along three diagnosis groups as follows: 99 CRSsNP patients, 172 CRSwNP patients, and 139 (non-CRS)  
160 controls. Beta diversity ordination plots (of weighted UniFrac and Jensen-Shannon distances) are shown  
161 in Figure 1. The plots do not reveal any distinct grouping by disease state or by centre, but on visual  
162 inspection show a triangular arrangement suggesting that samples lie on a continuum between three  
163 distinct clusters, providing motivation for further analysis.

## 164 Composition of the three sinonasal microbiotypes

165 We applied our microbiotyping approach through the unsupervised dimensionality reduction and  
166 clustering method described in the Methods. The composition of the resulting “sinonasal microbiotypes”  
167 is found in Figure 2A.



168  
169 **Figure 2: Microbiotyping the sinonasal microbiome. (A) Taxonomic composition of the three**  
170 **microbiotypes at the genus level. (B) Illustration of the assigned microbiotypes on the Jensen-Shannon**  
171 **PCoA biplot. Arrows were used to depict the projection of the genera onto the PCoA matrix. Each arrow**  
172 **is indicated by the color of the genus according to the Legend. (C) Histograms demonstrating the relative**

173 abundance of *Corynebacterium* and *Staphylococcus*. (D) Distribution of staphylococcal species (mean  
174 relative abundance). (E) Subgroups of microbiotype 3 (hierarchical density-based clustering).

175 Microbiotype 1 is dominated by *Corynebacterium* (mean relative abundance of 75.29%). Microbiotype 2  
176 is dominated by *Staphylococcus* (mean relative abundance of 74.96%). Microbiotype 3 contained samples  
177 that were mostly constituted of *Streptococcus*, *Haemophilus*, *Moraxella*, *Pseudomonas* and other genera.

178 The Abundance/Prevalence tables for the microbiotypes is demonstrated in Supplementary Tables [S1A](#),  
179 [S1B](#) and [S1C](#).

180 We used a PCoA biplot to project features (genera) onto the PCoA matrix.<sup>6</sup> The 5 topmost abundant  
181 genera were overlaid on the PCoA plot as arrows, originating from the centre of the plot and pointing to  
182 the direction of the projected feature coordinates. (Figure 2B) Each arrow is indicated by the color of the  
183 genus according to the Legend in Figure 2A, and the length of each was normalized as a percentage of the  
184 longest arrow. The coloring of the samples in 2B in the PCoA scatter plot according to the microbiotype  
185 assignment is provided for additional illustration. (Figure 2B) We note that the biplot arrows show a  
186 quasi-orthogonal arrangement between the key genera that constitute the microbiome.

187 The distributions of the relative adundances of *Corynebacterium* and *Staphylococcus* in all three  
188 microbiotypes were plotted in histograms (Figure 2C). It was noted that in microbiotype 1, most samples  
189 have a high abundance of Corynebacteria (i.e. Corynebacteria dominate), while Staphylococci appeared  
190 to dominate in microbiotype 2 in most samples.

## 191 Dissection of “sinonasal microbiotype 3”

192 We observed that Microbiotype 3 included various genera that did not cluster into the major two  
193 microbiotypes. It was also evident that this microbiotype is more heterogeneous. Applying the K-Means  
194 algorithm we showed poor clustering on only the first two and three Principal Components, since this  
195 group included multiple signatures with various dominant organisms. Accordingly, we employed the

196 hierarchical density-based clustering algorithm “hdbscan”<sup>7</sup> on the full-dimensional OTU table. One  
197 advantage of this algorithm is that it can estimate the number of clusters, without *a priori* specification by  
198 the user. This algorithm also has the ability to detect “outliers” that fail to cluster with the rest of the  
199 groups and detaches them into a separate “Miscellaneous/Other” group. We ran this algorithm on samples  
200 in Microbiotype 3 and this revealed four clusters, each dominated by one of the genera of *Streptococcus*  
201 (21 samples), *Haemophilus* (16 samples), *Moraxella* (9 samples), and *Pseudomonas* (7 samples), with a  
202 mean relative abundance ranging from 73.49% to 95.5%. The fifth cluster was the assigned  
203 “Miscellaneous/Other” group (18 samples). We term these “sub-microbiotypes”: microbiotype 3S, 3H,  
204 3M, 3P, and 3O, respectively. (Figure 2E)

205 **Exploring microbiotypes at the species-level reveals potential antagonism between**  
206 ***Corynebacterium* species and *Staphylococcus aureus***

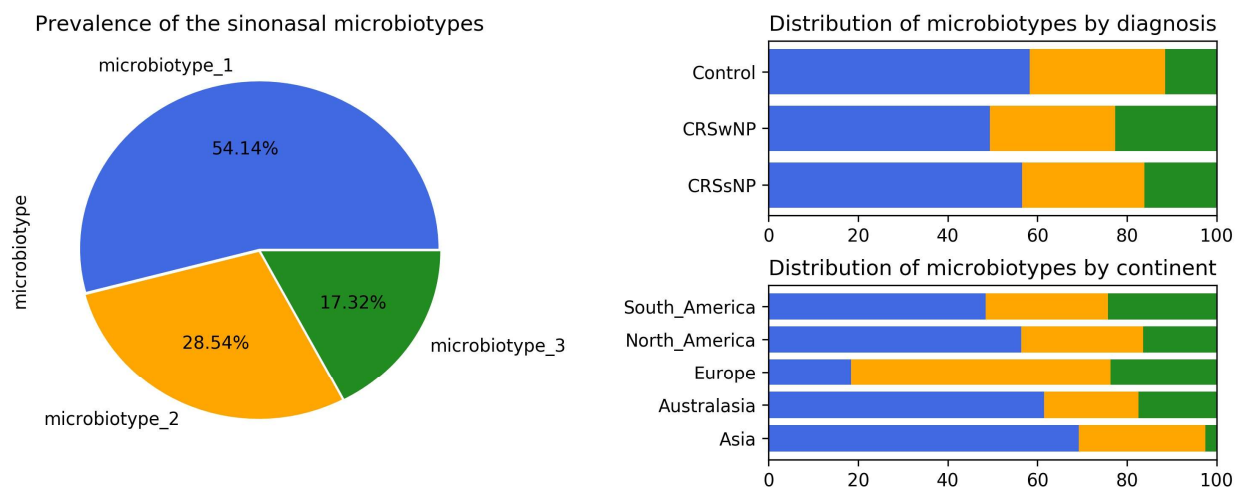
207 At present, species level assignment is limited by the current technology of 16S-surveys, the current state  
208 of microbial databases in general, and by our chosen short-read sequencing methodology. However,  
209 species level associations hold clinical significance for sinus health, since *Staphylococcus aureus* has  
210 been traditionally associated with biofilm formation and superantigen elaboration, both of which are  
211 associated with more severe sinus disease and poorer response to treatment. Furthermore nasal carriage of  
212 methicillin-resistant *Staphylococcus aureus* (MRSA) is a global health concern with implications that  
213 extend far beyond the sinuses. Moreover, our new QIIME 2-based pipeline<sup>8</sup> allows a higher “sub-OTU”  
214 resolution compared to older pipelines, offering an opportunity to resolve some taxa at species level when  
215 possible.<sup>9,10</sup>

216 We explored taxonomy assignment at the species level, with a focus on Staphylococcal species.  
217 Staphylococci were assigned to either *Staphylococcus aureus*, *Staphylococcus epidermidis* or unclassified  
218 *Staphylococcus*. We found that almost all of the assigned *Staphylococcus aureus* species were clustered in  
219 Microbiotype 2, forming 47.81% mean relative abundance of this Microbiotype, compared to 1.36% and  
220 0.3% in Microbiotype 1 and Microbiotype 3 respectively. (Figure 2E) Differential abundance of both

221 *Staphylococcus aureus* and *epidermidis* between the disease groups was confirmed as statistically  
222 significant using ANCOM.

223 In light of this finding, we hypothesized a reciprocal or antagonistic relationship between  
224 *Corynebacterium* sp. and *Staphylococcus aureus* and investigated this using SparCC. This confirmed a  
225 significant negative correlation between *Corynebacterium* genus and the species *Staphylococcus aureus*  
226 (SparCC correlation coefficient = -0.339, p = 0.001). Interestingly, *Staphylococcus epidermidis* positively  
227 correlated with *Corynebacterium* (SparCC correlation coefficient = 0.271, p = 0.001). These results  
228 should be interpreted cautiously in light of 16S-sequencing limitations. Nevertheless, they do appear to  
229 correlate to previous findings in the literature, including *in vitro* experiments<sup>11</sup>, a murine nasal bacterial  
230 interaction model<sup>12</sup>, and a survey of nasal vestibule swabs in healthy individuals<sup>13</sup>. These results suggest  
231 that a benign or probiotic role is played by both *Corynebacterium* spp. and *Staphylococcus epidermidis*  
232 when interacting with *Staphylococcus aureus*.

233 **Prevalence and distribution of the microbiotypes in different diagnoses and centres**



234

235 **Figure 3: Prevalence and distribution of the microbiotypes.**

236 Microbiotype 1 was assigned to 222 samples (54.1%), microbiotype 2 to 117 samples (28.5%), and  
237 microbiotype 3 to 71 samples (17.3%). The prevalence distribution of the sinonasal microbiotypes did not

238 appear to significantly differ by the disease state of the sinuses. (Figure 3) However, a Chi-Squared test  
239 on the contingency table by centre showed significantly different distributions by centre (FDR-corrected p  
240 < 0.001): there was a higher prevalence of microbiotype 2 in our European centre (Amsterdam), and a  
241 higher prevalence of microbiotype 1 in Asian and Australasian centres, with a much lower prevalence of  
242 microbiotype 3 in Asia. (Figure 3 and Table 1)

243 *Table 1: Distribution of microbiotypes by diagnosis and continent.*

variable	value	microbiotype_1	microbiotype_2	microbiotype_3	p value
Diagnosis	CRSsNP	56 (56.6%)	27 (27.3%)	16 (16.2%)	0.507
	CRSwNP	85 (49.4%)	48 (27.9%)	39 (22.7%)	
Continent	Control	81 (58.3%)	42 (30.2%)	16 (11.5%)	
Continent	Asia	27 (69.2%)	11 (28.2%)	1 (2.6%)	< 0.001
	Australasia	67 (61.5%)	23 (21.1%)	19 (17.4%)	
Continent	Europe	7 (18.4%)	22 (57.9%)	9 (23.7%)	
	North_America	89 (56.3%)	43 (27.2%)	26 (16.5%)	
Continent	South_America	32 (48.5%)	18 (27.3%)	16 (24.2%)	

244

## 245 **Associations of microbiotypes with clinical variables**

246 We then explore the distribution of the three microbiotypes among multiple clinical variables in Table 2.  
247 This shows no significant difference for some variables including asthma, aspirin sensitivity, GORD,  
248 diabetes mellitus, and current smoking status, (FDR-corrected p > 0.05; Chi-squared test). The cross  
249 tabulation however revealed a statistically significant association with “aspirin sensitivity” or aspirin-  
250 exacerbated respiratory disease (AERD) (p = 0.02), although this did not persist after a Benjamini-  
251 Hochberg correction (corrected p = 0.077). Patients who were aspirin-sensitive (or suffering from AERD)  
252 showed less prevalence of microbiotypes 1, 2 and a higher prevalence of microbiotype 3, compared to  
253 those who were not aspirin-sensitive. On the other hand, patients who were undergoing their “primary

254 surgery”, had a higher prevalence of microbiotype 1 and a lower prevalence of microbiotype 3, compared  
255 to those patients who had had previous surgeries, but these results were not statistically significant.

256 *Table 2: Distribution of microbiotypes by various clinical variables.*

variable	value	microbiotype_1	microbiotype_2	microbiotype_3	p value
Asthma	No	162 (56.4%)	81 (28.2%)	44 (15.3%)	0.906
	Yes	55 (51.4%)	31 (29.0%)	21 (19.6%)	
Aspirin sensitivity	No	202 (55.3%)	106 (29.0%)	57 (15.6%)	0.077
	Yes	12 (48.0%)	5 (20.0%)	8 (32.0%)	
Diabetes	No	189 (54.9%)	98 (28.5%)	57 (16.6%)	0.979
	Yes	22 (55.0%)	11 (27.5%)	7 (17.5%)	
GORD	No	177 (55.3%)	93 (29.1%)	50 (15.6%)	0.979
	Yes	35 (55.6%)	17 (27.0%)	11 (17.5%)	
Current Smoker	No	204 (54.4%)	110 (29.3%)	61 (16.3%)	0.077
	Yes	15 (57.7%)	4 (15.4%)	7 (26.9%)	
Primary surgery	No	92 (47.2%)	57 (29.2%)	46 (23.6%)	0.114
	Yes	130 (60.5%)	60 (27.9%)	25 (11.6%)	

257

258 **Validation of sinonasal microbiotyping on a separate dataset**

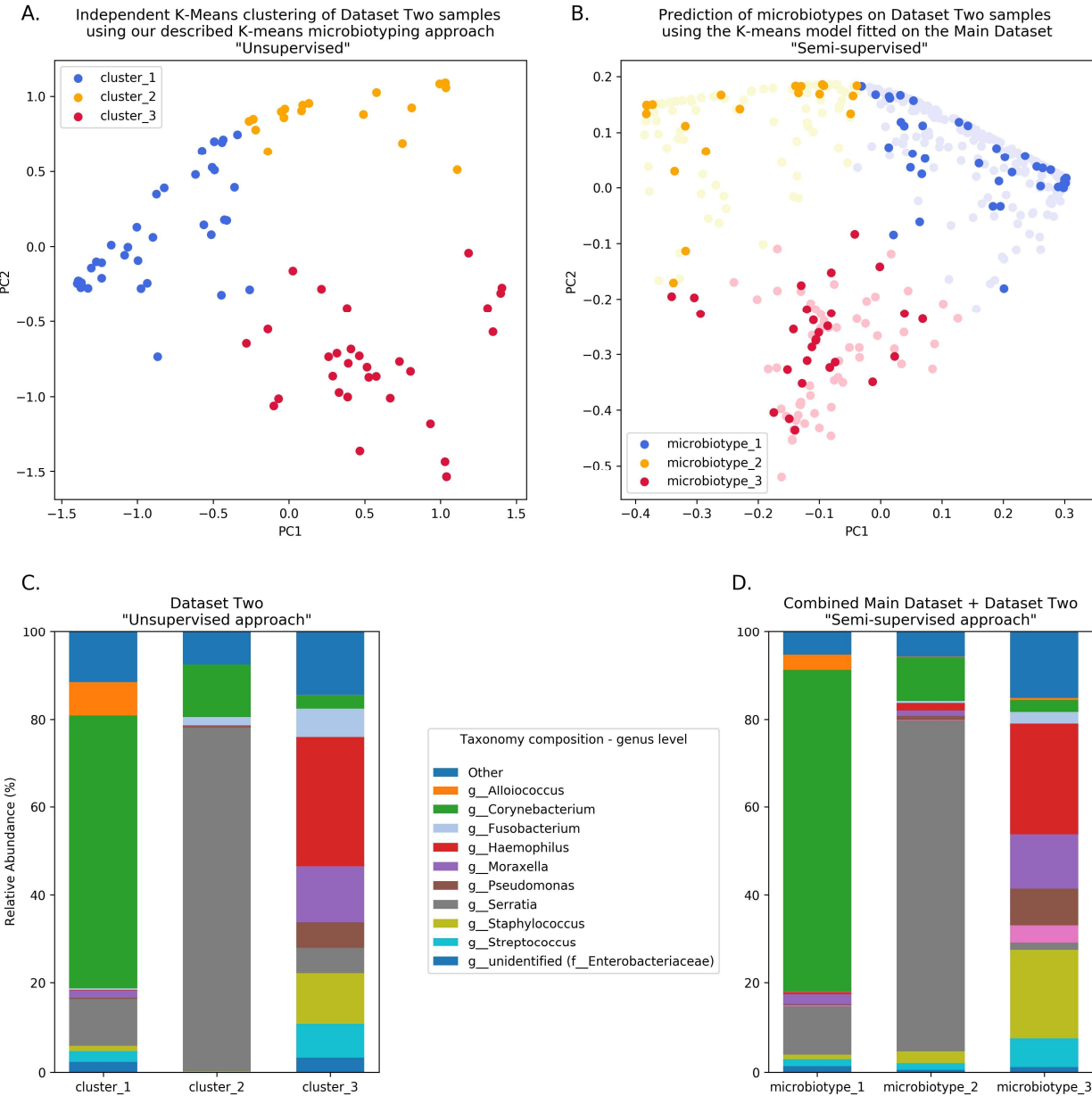
259 We validated our approach on a separate 16S dataset we called Dataset Two. As described in the Methods  
260 section, we validated this using an independent unsupervised approach and a semi-supervised approach  
261 guided by the Main Dataset.

262 The first unsupervised approach yielded three clusters similar to the microbiotypes described on the Main  
263 Dataset, with one cluster exhibiting high mean relative abundance of *Corynebacteria*, a second cluster  
264 exhibiting high mean relative abundance of *Staphylococcus*, and a third cluster with other dominant  
265 genera. Plotting the first two Principal Components (Figure 4A) resulting from PCoA on the JSD matrix  
266 revealed the same triangular distribution of samples observed in Figure 1.

267 Prevalence of the microbiotypes in this dataset (using the unsupervised approach) was as follows:  
268 microbiotype 1 assigned 39.2% of samples, microbiotype 2 with 26.8% of samples, and microbiotype 3  
269 with 34.0%.

270 The second semi-supervised approach yielded similar results (Figure 4; Supplementary Table), differing  
271 in the classification of only 3 samples (out of 97 samples; i.e. 3.09%). (See Supplementary Jupyter  
272 notebook) Two of these samples show *Staphylococcus* dominating the samples in combination with  
273 *Haemophilus*, with no overt dominance of one taxon over the other, making them more-or-less  
274 transitional samples between the signatures of microbiotypes 2 and 3. The third sample was dominated by  
275 *Staphylococcus* and *Corynebacterium*, making it a transitional sample between microbiotype 1 and  
276 microbiotype 2, with Staphylococcal species assigned to *epidermidis*, making this more appropriately  
277 assigned to microbiotype 1. (see Supplementary Jupyter notebook)

278 These results validate the microbiotyping approach and suggest that our approach and dataset could be  
279 used to guide classification of sinonasal samples sequenced in future separate studies. (Figure 4)  
280 Moreover, it points towards a potential clinical relevance of performing sinonasal microbiotyping.



281

282 **Figure 4: Validation of microbiotyping approach on Dataset Two.**

283

284 **DISCUSSION**

285 We demonstrate that the microbiota of most sinus swab samples could be classified into distinct  
286 signatures or archetypes, which we have termed “sinonasal microbiotypes”. We observed three main  
287 microbiotypes: the most prevalent being a *Corynebacterium*-dominated microbiotype (microbiotype 1),  
288 then a *Staphylococcus*-dominated microbiotype (microbiotype 2), and microbiotype 3 which includes  
289 samples dominated by *Streptococcus*, *Haemophilus*, *Moraxella*, *Pseudomonas*, and other genera (3S, 3H,  
290 3M, 3P, and 3O respectively).

291 As we have previously reported,<sup>2</sup> the sinus microbiota are dominated by the genera *Corynebacterium* and  
292 *Staphylococcus* (microbiotypes 1 and 2). A similar clustering approach to the sinus microbiome was  
293 applied by Cope and colleagues, who utilized Dirichlet multinomial mixture models (DMMs),<sup>5</sup> and  
294 reported that most samples in their study were occupied by a continuum of Staphylococcaceae and  
295 Corynebacteriaceae.<sup>5</sup> It appears that, regardless the statistical or clustering methodology utilized, it is  
296 most likely that the sinonasal microbiome consists of core organisms<sup>2</sup> that have a distinct co-occurrence  
297 pattern. This could be explored through a network analysis approach and should be a future area of study.

298 *Staphylococcus aureus* has been perceived to be an important pathogen in sinus inflammatory disease.  
299 *Staphylococcus aureus* biofilms may act as a nidus for recurrent infections<sup>14,15</sup> and as a “nemesis” of  
300 otherwise-successful sinus surgery.<sup>16–18</sup> *Staphylococcus aureus* is also a producer of exotoxins, which in  
301 some cases can serve as superantigens, and these have been previously described as playing an important  
302 role in the pathogenesis of CRSwNP.<sup>19</sup> *Pseudomonas aeruginosa* biofilms are also virulent organisms that  
303 are difficult to eradicate from the sinuses, and have been associated with worse clinical outcomes.<sup>20</sup> Both  
304 these organisms are important pathogens in the chronic mucociliary dysfunction exhibited in cystic  
305 fibrosis. However, methicillin-resistant *Staphylococcus aureus* (MRSA) is an important nasal colonizer  
306 that could asymptotically colonize the nose. What determines the clinical course, between  
307 asymptomatic colonization versus symptomatic pathogenicity, remains an interesting topic of research. In

308 this study, we identified a potential reciprocal relationship between *Staphylococcus aureus* and  
309 *Corynebacterium*. Being aware of the challenges of compositional data analysis, we utilized for this  
310 purpose the specialized SparCC algorithm which infers correlations from compositional data.<sup>21</sup> This  
311 finding needs to be supported by future co-culture experiments, but suggests that *Corynebacterium* sp.  
312 may be a “cornerstone” of sinus microbial health. It is important to note that our bioinformatic  
313 methodology has been intentionally designed to utilize state-of-the-art software methods at every step of  
314 the analysis pipeline, in order to maximise the resolution of taxonomy assignment.<sup>8,9,22</sup> Nevertheless, our  
315 approach is still confined within the limitations of current 16S sequencing methodologies, and the  
316 confidence of assignment is reduced beyond the genus level. Our analysis pipeline could not delineate  
317 between different *Corynebacterium* at the species level and *Staphylococcus aureus* at the strain level.  
318 Hence functional difference between samples with same species remain to be determined using a  
319 functional metagenomics approach. A recent study suggest that by incorporating location information or  
320 “sample-level metadata” into species-level assignment accuracy could be improved.<sup>23</sup> In our study, the  
321 differential relationships of both *Staphylococcus aureus* and *epidermidis* towards *Corynebacteria*  
322 (negative and positive associations, respectively) could be of clinical significance and is worthy of future  
323 investigation. We performed a post-hoc inspection of species-level assignment in Dataset Two, to  
324 investigate whether this finding will be reproducible in a separate dataset. This confirmed clustering of  
325 almost all *Staphylococcus aureus* species in microbiotype 2. (Supplementary Results in Jupyter  
326 Notebook)

327 Interestingly, we found that the distribution of the sinonasal microbiotypes was not significantly dis-  
328 similar amongst healthy controls and CRS patients. There appeared to be no significant associations with  
329 other clinical variables such as asthma and aspirin-sensitivity after controlling for multiple comparisons.  
330 (Table 2) The distribution of the microbiotypes however differed according to centre/location of  
331 collection. (Figure 3) As such, we cannot conclude based on our study that microbiotypes could function  
332 independently as a disease biomarker. Although not reaching statistical significance (chi squared p >

333 0.05) the prevalence of microbiotype 3 was higher in CRSsNP and CRSwNP, compared to controls. It  
334 could be the case that chronicity of inflammation -on its own- is not a determinant of a dysbiotic  
335 microbiome, but whether there is a clinically-evident “sinus infection” current at the time of sample  
336 collection. In this theory, stable chronic sinuses with no overt signs of acute or chronic infection, may  
337 remain similar to a “healthy sinus microbiome”. Only when the sinuses are clinically infected (as evident  
338 on clinical symptoms and endoscopic findings), the microbiota become disrupted and the dysbiosis  
339 exaggerated. It is important to note that *Streptococcus*, *Haemophilus* and *Moraxella* (represented here in  
340 microbiotype 3) have been traditionally implicated in acute infections of the upper respiratory tract  
341 including acute rhinosinusitis and acute otitis media. Unfortunately, information regarding acute  
342 exacerbations was not explored within this study.

343 Regarding geographical differences: Asia and Australasia showed an over-representation of microbiotype  
344 1. Europe had a higher prevalence of microbiotype 2. Unfortunately, the study only included one  
345 European centre (Amsterdam) so it is difficult to be certain whether this finding generalizes to other  
346 locations in Europe. The driving factors for these geographical differences could be multiple, including  
347 but not limited to clinical practices such as local antibiotic prescriptions for CRS and timing of  
348 recruitment of patients for sinus surgery, as discussed previously.<sup>2</sup>

349 We have adapted our methodology from the enterotyping approach taken by Arumugam et al.<sup>4</sup> for  
350 classifying bacterial signatures of the gut microbiome. In their original manuscript, they described three  
351 different enterotypes in the gut dominated by *Prevotella*, *Bacteroidetes*, and *Ruminococcus* respectively.<sup>4</sup>  
352 Several papers have correlated gut enterotypes with various clinical variables.<sup>24,25</sup> Despite this,  
353 enterotyping as an approach to population stratification has not been without its controversies. Several  
354 authors have criticized the definition of distinct clusters, since it neglects intra-cluster variation and  
355 gradients between clusters.<sup>26-29</sup> We provide answers to previous critique<sup>28</sup> to enterotyping as it applies to  
356 our study in Supplementary Table S2. It is important to note these valid criticisms to any community  
357 typing approach. In our experiment, the clusters or types lie on a continuum, with some samples falling in

358 the gradients between two, or perhaps even all three microbiotypes (see ordination plots). The histograms  
359 in Figure 2 also suggest this, but they do show most samples in each microbiotype feature a high relative  
360 abundance of a dominating genus in many samples. We investigated a simple dominance measure, the  
361 Berger-Parker (BP) alpha diversity index,<sup>30</sup> in the combined datasets' 507 samples. The Berger-Parker  
362 index simply reports the relative abundance of the most dominant taxon in a sample. This found that only  
363 24.9% of samples had a dominating taxon that only had a relative abundance of 50% or less. On the other  
364 hand, 51.9% of samples had the dominant taxon exhibiting a relative abundance of greater than 70% of  
365 the sample.(Supplementary Results in Jupyter notebook; Supplementary Figure S1) This shows that in  
366 most samples, there is one dominating organism. Based on these results, the microbiotyping approach is  
367 therefore proposed to reduce complexity about modeling bacterial interactions in the sinuses, and not to  
368 suggest that each type is a walled-off discrete cluster. Further investigations into the local substructures of  
369 each type will be required to further explore the roles and interactions of its constituent taxa. Another  
370 limitation of our description of microbiotypes is that they may as well describe different community  
371 "states" rather than community "types", since we do not have longitudinal data to describe how these  
372 clusters behave with the passage of time and treatments. Hence, we could not confirm whether these are  
373 stable, consistent communities across time. It may well be that intermediate samples lying between two or  
374 more microbiotypes are representing a transitional state. An important future avenue of research is to  
375 conduct a longitudinal study to investigate the temporal stability of these clusters.

376 We predict that ongoing sinonasal microbiome research and consequent large meta-analyses of  
377 microbiota studies, with novel tools (such as QIITA<sup>31</sup>) enabling such large-scale studies, will allow the  
378 refinement of these types and further clarify their clinical/microbiological utility. Our methodological  
379 approach to describe the microbiotypes is not exclusive, as alternative statistical or machine-learning  
380 approaches could be employed to investigate them. In light of this, we expect that international multi-  
381 centre standardization and rationalization of the sinonasal microbiotypes would be possible in the future,  
382 similar to the recent proposed effort to standardize enterotyping of the gut microbiota by Costea et al.<sup>29</sup>

383 **CONCLUSION**

384 We investigated the ISMS dataset through an approach modeled on human gut microbiome enterotyping  
385 and we found three major microbial community types or “microbiotypes” as clusters that lie on a  
386 continuum, based on an unsupervised machine learning approach that involved dimensionality reduction  
387 and clustering. Microbiotypes did not show an association with disease state or clinical variable,  
388 suggesting that they could not function as independent disease biomarkers. The description of these  
389 microbiotypes has also unveiled a potential reciprocal relationship between *Staphylococcus aureus* and  
390 *Corynebacterium spp.* in the sinuses that requires further investigation in future studies. The findings  
391 were validated on a separate previously unpublished sinus bacterial 16S gene dataset. Microbiotypes are  
392 therefore proposed to reduce the complexity of modeling bacterial interactions in the sinuses, and in this  
393 sense hold microbiological and clinical relevance that could potentially influence medical and surgical  
394 treatment of CRS patients.

395

396 **METHODS**

397 **The “International Sinonasal Microbiome Study (ISMS)” dataset**

398 We perform the primary analysis on the dataset obtained from the “International Sinonasal Microbiome  
399 Study (ISMS)” project.<sup>2</sup> In summary, this dataset is a multi-centre 16S-amplicon dataset which includes  
400 endoscopically-guided, guarded swabs collected from the sinuses (in particular the middle meatus /  
401 anterior ethmoid region) of 532 participants in 13 centres representing 5 continents. Details of sample  
402 collection, DNA extraction and sequencing methodologies are described in the original report.<sup>2</sup> The 16S  
403 gene region sequenced was the V3–V4 hypervariable region, utilizing primers  
404 (CCTAYGGGRBGCASCAG forward primer) and (GGACTACNNGGTATCTAAT reverse primer)  
405 according to protocols at the sequencing facility (the Australian Genome Research Facility; AGRF).  
406 Sequencing was done on the Illumina MiSeq platform (Illumina Inc., San Diego, CA) with 300-base-pairs  
407 paired-end Illumina chemistry

408 **Bioinformatics pipeline**

409 Details of the bioinformatic pipeline is detailed in the original report.<sup>2</sup> In summary, we utilized a QIIME  
410 2-based pipeline.<sup>8</sup> Forward and reverse fastq reads were joined<sup>32</sup>, quality-filtered,<sup>33</sup>, abundance-filtered<sup>34</sup>,  
411 then denoised using deblur<sup>9</sup> through QIIME 2-based plugins. This yielded a final feature table of high-  
412 quality, high-resolution Amplicon Sequence Variants (ASVs). Taxonomy assignment and phylogenetic  
413 tree generation<sup>35</sup> was done against the Greengenes<sup>36</sup> database; and taxonomy was assigned using the  
414 QIIME 2 BLAST assigner.<sup>22</sup> A rarefaction minimum depth cut-off was chosen at 400 and this yielded 410  
415 samples out of the original 532 for downstream analysis. The same pipeline was then applied on DataSet  
416 Two for purposes of validation of microbiotyping. We chose to reproduce exactly all the original pipeline  
417 steps on DataSet Two, despite being a completely separate dataset, to reduce bias.

418 **Delineating the microbiotypes of the sinonasal microbiome**

419 Our approach was guided by the “enterotyping” method described by Arumugam et al.<sup>4</sup> with adaptations.  
420 We constructed a sample distance matrix using the Jensen-Shannon distance (JSD) metric, as used in the  
421 original “enterotypes” paper.<sup>4</sup> The Jensen-Shannon distances were calculated between samples in the  
422 genus-level-assigned table in a pairwise fashion using the JSD function in the R package “philentropy”  
423 with a log ( $\log_{10}$ ) base. Following this, Principal Coordinate analysis (PCoA) was done on the distance  
424 matrix for dimensionality reduction and visualization. Clustering was then performed using a standard K-  
425 means clustering algorithm, as implemented in the machine learning Python package scikit-learn (version  
426 0.20.1);<sup>37</sup>) on the first two principal components (PCs) obtained from the PCoA, with the number of  
427 clusters (k) chosen at 3 based on visual inspection of the beta diversity PCoA plots. Average silhouette  
428 scores, as implemented in scikit-learn, for the range (k = 2 - 8) were calculated to assess clustering  
429 quality, and this revealed the highest silhouette scores: 0.61 and 0.6 for [k=4] and [k=3] respectively. The  
430 three resulting clusters were defined as the three sinonasal microbiotypes. For further exploration of the  
431 subgroups that constitute microbiotype 3, we used the hierarchical density-based clustering algorithm  
432 “hdbscan”<sup>7</sup> on the full-dimensional feature table. Genera were projected onto the PCoA matrix using a  
433 biplot approach<sup>6</sup>, as implemented in scikit-bio’s function “*pcoa\_biplot*”. Genera were represented in the  
434 biplot figure as arrows, originating from the centre of the plot pointing to the direction of the projected  
435 feature coordinates, and the lengths normalized as a percentage of the longest arrow. We utilized  
436 “Analysis of Compositions of Microbiomes (ANCOM)”<sup>38</sup> for identifying differentially-abundant taxa.  
437 Taxa genus level and *Staphylococcus* species level co-occurrence/correlation analysis were done after  
438 taxonomy assignment using SparCC algorithm,<sup>21</sup> in the fast implementation in FastSpar.<sup>39</sup>

439 **Validating microbiotypes on a second sinonasal microbiome dataset**

440 To infer whether our classification could be generalizable to other sinonasal microbiome samples not  
441 included in this study, we sought to validate our microbiotyping approach on a separate, previously-  
442 unpublished, 16S dataset. This dataset includes sinonasal microbiome swabs collected from private and

443 public patients attending the Otolaryngology Department (University of Adelaide) to have surgery done  
444 by the authors P.J.W., A.J.P. or the Otorhinolaryngology Service at the Queen Elizabeth Hospital in  
445 Adelaide, South Australia. Similar to the main dataset, these included CRS patients who underwent  
446 endoscopic sinus surgery for this sinus disease, and non-CRS control patients who underwent other  
447 otolaryngological procedures, such as tonsillectomy, septoplasty or skullbase tumour resection. Sample  
448 collection, and processing were done in a standardized fashion similar to that has been described in the  
449 ISMS main dataset, except that DNA extraction was carried out using the PowerLyzer Power-Soil DNA  
450 kit (MoBio Laboratories, Salona Beach, CA) as previously described<sup>40</sup>, rather than the Qiagen DNeasy kit  
451 (Qiagen, Hilden, Germany). Similar to the ISMS samples, library preparation and 16S sequencing were  
452 done at the Australian Genome Research Facility (AGRF) on the Illumina MiSeq platform (Illumina Inc.,  
453 San Diego, CA, USA) with the 300-base-pairs paired-end chemistry. Libraries were generated by  
454 amplifying (341F–806R) primers against the V3–V4 hypervariable region of the 16S gene  
455 (CCTAYGGGRBGCASCAG forward primer; GGACTACNNGGTATCTAAT reverse primer).<sup>41</sup> PCR  
456 was done using AmpliTaq Gold 360 master mix (Life Technologies, Mulgrave, Australia) following a  
457 two-stage PCR protocol (29 cycles for the first stage; and 8 cycles for the second, indexing stage).  
458 Sequencing was done over two MiSeq runs in January 2015. We termed this dataset in this manuscript  
459 “Dataset Two”. This dataset comprises samples collected from 129 participants. Rarefaction at a cutoff of  
460 400 reads was performed, to match what was performed for the main dataset, and samples with read  
461 number less than 400 were excluded; this yielded a final feature table containing 97 samples, representing  
462 33 CRSsNP patients, 35 CRSwNP patients, and 29 controls.

463 We took two separate approaches to validation. The first approach is to replicate the previously-described  
464 unsupervised K-means microbiotyping methodology independently on samples in Dataset Two. We call  
465 this first approach the “unsupervised approach”. The second approach is to use the K-means model that  
466 was fitted on the samples from the Main Dataset to predict labels (i.e. microbiotypes) of the samples in

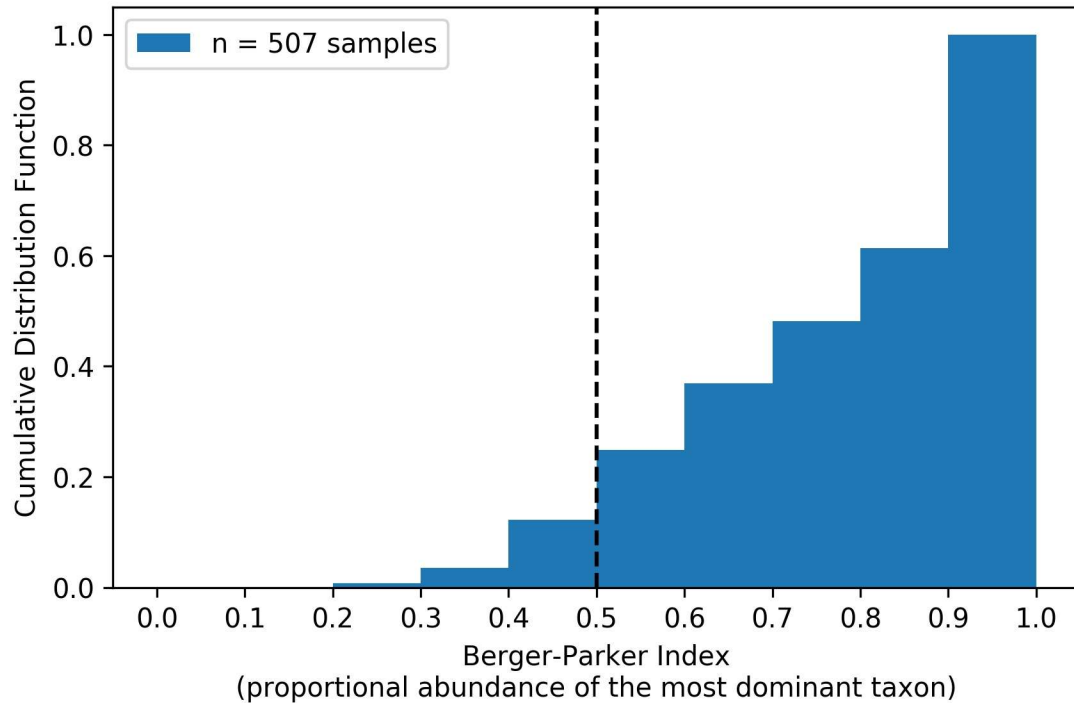
467    Dataset Two. As such, the Main Dataset is used as a “training dataset” in the language of machine  
468    learning. We called the second approach the “semi-supervised approach”.

469    **Statistical Analysis**

470    All frontend analyses were done using the Jupyter notebook frontend<sup>42</sup> and utilizing the assistance of  
471    packages from the Scientific Python<sup>43</sup> stack (numpy, scipy, pandas, statsmodels), scikit-learn<sup>37</sup>, scikit-bio  
472    (<https://github.com/biocore/scikit-bio>) and omicexperiment  
473    (<https://www.github.com/bassio/omicexperiment>).

474

475 **Supplementary Figures**



476

477 **Figure S1: Cumulative distribution function of the Berger-Parker Index in the combined datasets.**

478

479 **Supplementary Tables**

480 *Table S1A: Predominant taxa of microbiotype 1.*

genus	Mean Relative Abundance (%)	Prevalence (%)
Corynebacterium	75.29	100
Staphylococcus	10.69	76.58
Alloiococcus	2.79	28.83
Moraxella	2.31	9.91
unidentified (Enterobacteriaceae)	1.41	15.32
unidentified (Neisseriaceae)	1.18	20.72
Streptococcus	1	21.62
Haemophilus	0.56	9.91
unidentified (Moraxellaceae)	0.44	2.7
Ralstonia	0.34	10.36

481

482 *Table S1B: Predominant taxa of microbiotype 2.*

genus	Mean Relative Abundance (%)	Prevalence (%)
Staphylococcus	74.96	100
Corynebacterium	9.87	64.1
Streptococcus	3.22	25.64
unidentified (Enterobacteriaceae)	1.82	15.38
Haemophilus	1.41	10.26
Moraxella	1.27	5.13
Ralstonia	1.19	11.97
Pseudomonas	1.05	6.84
Parvimonas	0.72	0.85
unidentified (Neisseriaceae)	0.61	7.69

483

484 *Table S1C: Predominant taxa of microbiotype 3.*

genus	Mean Relative Abundance (%)	Prevalence (%)
Haemophilus	23.78	40.85
Streptococcus	23.22	46.48
Moraxella	12.11	19.72
Pseudomonas	9.17	15.49
unidentified (Enterobacteriaceae)	5.74	9.86
Serratia	5.7	8.45
Klebsiella	2.75	4.23
Corynebacterium	2.56	46.48
Prevotella	1.44	12.68
Acinetobacter	1.38	1.41

485

486 *Table S2: Addressing previous criticism to gut enterotyping.*

Critique	Answer
Discrete clusters or a multi-dimensional gradient?	We acknowledge the a proportion of samples fall in the gradient between the proposed microbiotypes. Berger-Parker index investigation showed that most samples had one dominating taxon.
Do discrete clusters link to human disease?	No. We report that we could not find an association between the microbiotype and chronic sinusitis disease status.
Is sampling frame or selection bias affecting results?	No; Multi-centre international study with consecutive sampling methodology. We also validate on a separate dataset.
Use inappropriate visualization such as “star-burst plots”?	We did not use inappropriate visualizations.
Use a supervised approach “between-class analysis”?	We use an unsupervised clustering and dimensionality reduction approach.
Is an individual’s microbiotype stable over time?	Answer unknown; Future longitudinal studies required.

487

## 488 REFERENCES

- 489 1. Fokkens, W. J. *et al.* EPOS 2012: European position paper on rhinosinusitis and nasal polyps 2012. A  
490 summary for otorhinolaryngologists. *Rhinology* **50**, 1–12 (2012).
- 491 2. Paramasivan, S. *et al.* The international sinonasal microbiome study (ISMS): A multi centre,  
492 international characterization of sinonasal bacterial ecology. *bioRxiv* 548743 (2019). doi:[10.1101/548743](https://doi.org/10.1101/548743)
- 493 3. Wagner Mackenzie, B. *et al.* Bacterial community collapse: A meta-analysis of the sinonasal  
494 microbiota in chronic rhinosinusitis. *Environmental Microbiology* **19**, 381–392 (2017).
- 495 4. Arumugam, M. *et al.* Enterotypes of the human gut microbiome. *Nature* **473**, 174–180 (2011).
- 496 5. Cope, E. K., Goldberg, A. N., Pletcher, S. D. & Lynch, S. V. Compositionally and functionally distinct  
497 sinus microbiota in chronic rhinosinusitis patients have immunological and clinically divergent  
498 consequences. *Microbiome* **5**, 53 (2017).
- 499 6. Legendre, P. & Legendre, L. *Numerical ecology*. (Elsevier, 2012).
- 500 7. McInnes, L., Healy, J. & Astels, S. HdbSCAN: Hierarchical density based clustering. *The Journal of*  
501 *Open Source Software* **2**, 205 (2017).
- 502 8. Bolyen, E. *et al.* QIIME 2: Reproducible, interactive, scalable, and extensible microbiome data  
503 science. (PeerJ Inc., 2018). doi:[10.7287/peerj.preprints.27295v1](https://doi.org/10.7287/peerj.preprints.27295v1)
- 504 9. Amir, A. *et al.* Deblur Rapidly Resolves Single-Nucleotide Community Sequence Patterns. *mSystems*  
505 **2**,
- 506 10. Thompson, L. R. *et al.* A communal catalogue reveals Earth's multiscale microbial diversity. *Nature*  
507 **551**, 457–463 (2017).
- 508 11. Barrow, G. I. Microbial Antagonism by *Staphylococcus aureus*. *Microbiology* **31**, 471–481 (1963).
- 509 12. Cleland, E. J. *et al.* Probiotic manipulation of the chronic rhinosinusitis microbiome. *International*  
510 *Forum of Allergy & Rhinology* **4**, 309–314 (2014).
- 511 13. Lina, G. *et al.* Bacterial competition for human nasal cavity colonization: Role of Staphylococcal agr  
512 alleles. *Applied and Environmental Microbiology* **69**, 18–23 (2003).
- 513 14. Jervis-Bardy, J., Foreman, A., Boase, S., Valentine, R. & Wormald, P.-J. What is the origin of  
514 *Staphylococcus aureus* in the early postoperative sinonasal cavity? *International Forum of Allergy &*  
515 *Rhinology* **1**, 308–312
- 516 15. Drilling, A. *et al.* Cousins, siblings, or copies: The genomics of recurrent *Staphylococcus aureus*  
517 infections in chronic rhinosinusitis. *International Forum of Allergy & Rhinology* **4**, 953–960 (2014).
- 518 16. Psaltis, A. J., Weitzel, E. K., Ha, K. R. & Wormald, P.-J. The effect of bacterial biofilms on post-  
519 sinus surgical outcomes. *American Journal of Rhinology* **22**, 1–6
- 520 17. Foreman, A. & Wormald, P.-J. Different biofilms, different disease? A clinical outcomes study. *The*  
521 *Laryngoscope* **120**, 1701–1706 (2010).

522 18. Singhal, D., Foreman, A., Bardy, J.-J. & Wormald, P.-J. *Staphylococcus aureus* biofilms: Nemesis of  
523 endoscopic sinus surgery. *The Laryngoscope* **121**, 1578–1583 (2011).

524 19. Bachert, C., Zhang, N., Patou, J., van Zele, T. & Gevaert, P. Role of staphylococcal superantigens in  
525 upper airway disease. *Current Opinion in Allergy and Clinical Immunology* **8**, 34–38 (2008).

526 20. Bendouah, Z., Barbeau, J., Hamad, W. A. & Desrosiers, M. Biofilm formation by *Staphylococcus*  
527 *aureus* and *Pseudomonas aeruginosa* is associated with an unfavorable evolution after surgery for chronic  
528 sinusitis and nasal polyposis. *Otolaryngology–Head and Neck Surgery: Official Journal of American*  
529 *Academy of Otolaryngology-Head and Neck Surgery* **134**, 991–996 (2006).

530 21. Friedman, J. & Alm, E. J. Inferring Correlation Networks from Genomic Survey Data. *PLOS*  
531 *Computational Biology* **8**, e1002687 (2012).

532 22. Bokulich, N. A. *et al.* Optimizing taxonomic classification of marker-gene amplicon sequences with  
533 QIIME 2's q2-feature-classifier plugin. *Microbiome* **6**, 90 (2018).

534 23. Kaehler, B. D., Bokulich, N., Caporaso, J. G. & Huttley, G. A. Species-level microbial sequence  
535 classification is improved by source-environment information. *bioRxiv* 406611 (2018).  
536 doi:[10.1101/406611](https://doi.org/10.1101/406611)

537 24. Wu, G. D. *et al.* Linking long-term dietary patterns with gut microbial enterotypes. *Science (New*  
538 *York, N.Y.)* **334**, 105–108 (2011).

539 25. Vandeputte, D. *et al.* Stool consistency is strongly associated with gut microbiota richness and  
540 composition, enterotypes and bacterial growth rates. *Gut* **65**, 57–62 (2016).

541 26. Jeffery, I. B., Claesson, M. J., O'Toole, P. W. & Shanahan, F. Categorization of the gut microbiota:  
542 Enterotypes or gradients? *Nature Reviews. Microbiology* **10**, 591–592 (2012).

543 27. Koren, O. *et al.* A Guide to Enterotypes across the Human Body: Meta-Analysis of Microbial  
544 Community Structures in Human Microbiome Datasets. *PLOS Computational Biology* **9**, e1002863  
545 (2013).

546 28. Knights, D. *et al.* Rethinking 'Enterotypes'. *Cell host & microbe* **16**, 433–437 (2014).

547 29. Costea, P. I. *et al.* Enterotypes in the landscape of gut microbial community composition. *Nature*  
548 *Microbiology* **3**, 8–16 (2018).

549 30. Berger, W. H. & Parker, F. L. Diversity of planktonic foraminifera in deep-sea sediments. *Science*  
550 *(New York, N.Y.)* **168**, 1345–1347 (1970).

551 31. Gonzalez, A. *et al.* Qiita: Rapid, web-enabled microbiome meta-analysis. *Nature Methods* **15**, 796–  
552 798 (2018).

553 32. Zhang, J., Kobert, K., Flouri, T. & Stamatakis, A. PEAR: A fast and accurate Illumina Paired-End  
554 reAd mergeR. *Bioinformatics* **30**, 614–620 (2014).

555 33. Bokulich, N. A. *et al.* Quality-filtering vastly improves diversity estimates from Illumina amplicon  
556 sequencing. *Nature Methods* **10**, 57–59 (2013).

557 34. Wang, J. *et al.* *Minimizing spurious features in 16S rRNA gene amplicon sequencing.* (PeerJ Inc.,  
558 2018). doi:[10.7287/peerj.preprints.26872v1](https://doi.org/10.7287/peerj.preprints.26872v1)

559 35. Janssen, S. *et al.* Phylogenetic Placement of Exact Amplicon Sequences Improves Associations with  
560 Clinical Information. *mSystems* **3**,

561 36. DeSantis, T. Z. *et al.* Greengenes, a Chimera-Checked 16S rRNA Gene Database and Workbench  
562 Compatible with ARB. *Applied and Environmental Microbiology* **72**, 5069–5072 (2006).

563 37. Pedregosa, F. *et al.* Scikit-learn: Machine Learning in Python. *Journal of Machine Learning Research*  
564 **12**, 2825–2830 (2011).

565 38. Mandal, S. *et al.* Analysis of composition of microbiomes: A novel method for studying microbial  
566 composition. *Microbial Ecology in Health and Disease* **26**, 27663 (2015).

567 39. Watts, S. C., Ritchie, S. C., Inouye, M. & Holt, K. E. FastSpar: Rapid and scalable correlation  
568 estimation for compositional data. *bioRxiv* 272583 (2018). doi:[10.1101/272583](https://doi.org/10.1101/272583)

569 40. Chan, C. L. *et al.* The microbiome of otitis media with effusion. *The Laryngoscope* **126**, 2844–2851  
570 (2016).

571 41. Yu, Y., Lee, C., Kim, J. & Hwang, S. Group-specific primer and probe sets to detect methanogenic  
572 communities using quantitative real-time polymerase chain reaction. *Biotechnology and Bioengineering*  
573 **89**, 670–679 (2005).

574 42. Kluyver, T. *et al.* Jupyter Notebooks a publishing format for reproducible computational workflows.  
575 in *Positioning and Power in Academic Publishing: Players, Agents and Agendas* (eds. Loizides, F. &  
576 Scmidt, B.) 87–90 (IOS Press, 2016). doi:[10.3233/978-1-61499-649-1-87](https://doi.org/10.3233/978-1-61499-649-1-87)

577 43. Oliphant, T. E. Python for Scientific Computing. *Computing in Science & Engineering* **9**, 10–20  
578 (2007).